Original Article

Screening of the novel immune-suppressive biomarkers of TMED family and whether knockdown of TMED2/3/4/9 inhibits cell migration and invasion in breast cancer

Zheng Fang[1#], Yu-Xin Song[1#], Guan-Qun Wo[2#], Hong-Lei Zhou[1], Lei Li[1], Si-Yuan Yang[1], Xiu Chen[1], Jian Zhang[1], Jin-Hai Tang[1]^

[1]Department of General Surgery, the First Affiliated Hospital of Nanjing Medical University, Nanjing, China; [2]The First Clinical Medical College, Nanjing University of Chinese Medicine, Nanjing, China

Contributions: (I) Conception and design: Z Fang, JH Tang; (II) Administrative support: HL Zhou, JH Tang; (III) Provision of study materials or patients: X Chen, J Zhang, JH Tang; (IV) Collection and assembly of data: Z Fang, YX Song, HL Zhou, L Li, GQ Wo, SY Yang, J Zhang; (V) Data analysis and interpretation: Z Fang, YX Song, HL Zhou, L Li, GQ Wo, SY Yang, J Zhang; (VI) Manuscript writing: All authors; (VII) Final approval of manuscript: All authors.

[#]These authors have contributed equally to this work and should be considered as co-first authors.

Correspondence to: Jin-Hai Tang; Jian Zhang. Department of General Surgery, the First Affiliated Hospital of Nanjing Medical University, 300 Guangzhou Road, Nanjing 210029, China. Email: jhtang@njmu.edu.cn; dr_jianzhang@njmu.edu.cn.

Background: Transmembrane p24 trafficking protein (TMED) family members are implicated in several solid tumors, but their clinical relevance for breast cancer (BC) remains unclear. This study aimed to probe their prognostic values and relations with tumor immunity in BC.

Methods: TMED family mRNA expression was assessed in five microarray datasets (GSE65212, GSE42568, GSE5364, GSE22820 and GSE45827) from Gene Expression Omnibus (GEO) database and invasive breast cancer (BRCA) cohort from The Cancer Genome Atlas (TCGA). Receiver operating characteristic (ROC) curve was performed to determine the predictive values of filtered members of the *TMED* family. The protein expressions of screen genes were validated by Clinical Proteomic Tumor Analysis Consortium (CPTAC) data from University of ALabama at Birmingham CANcer data analysis portal (UALCAN) and detected in the clinical specimens by western blot assay. Clinicopathologic variables were analyzed with bc-GenExMiner, and patient prognostic data were obtained with Kaplan-Meier Plotter. *In vitro* wound healing and invasion assays were performed on siRNA-transfected BC cell lines. TIMER 2.0, SangerBox, and ImmPort were used to evaluate tumor immune infiltration, immune checkpoints, and other immune-related genes. CbioPortal, Metascape, Expression2kinases, and LinkedOmics were used to explore gene regulatory network.

Results: BC tissues expressed *TMED*2/3/4/9 at a higher level than normal tissues, providing diagnostic potential. All the areas under the ROC curve for *TMED*2/3/4/9 were more than 0.7. *TMED*2/3/4/9 correlated with numerous clinical variables, including lymph node status, Scarff-Bloom-Richardson score (SBR), Nottingham Prognostic Index (NPI), estrogen receptor (ER), progesterone receptor (PR), human epidermal growth factor receptor 2 (HER-2), and triple-negative breast cancer (TNBC) status, and their high expression predicted the poor prognosis of BC patients. *TMED*2/3/4/9 knockdown drastically inhibited the migratory and invasive capacities of MDA-MB-231 and HCC1937 cells. *TMED*2/3/4/9 expressions correlated negatively with the infiltration of tumor-suppressive immune cells such as $CD8^+$ T cells, dendritic cells, and natural killer cells, and was inversely related to a variety of immune checkpoint genes, including programmed cell death 1 (*PD-1*) and cytotoxic T-lymphocyte associated protein 4 (*CTLA4*). A set of kinases, transcription factors, and microRNAs (miRNAs) may regulate TMED2/3/4/9 abnormalities at the genome level.

^ ORCID: 0000-0003-2016-4216.

Conclusions: *TMED2/3/4/9* may serve as diagnostic, prognostic, and immune-suppressive biomarkers in BC.

Keywords: TMED family; breast cancer; biomarkers; clinical relevance; tumor immunity

Submitted Oct 14, 2022. Accepted for publication Dec 07, 2022.
doi: 10.21037/atm-22-5444
View this article at: https://dx.doi.org/10.21037/atm-22-5444

Introduction

Breast cancer (BC) accounted for 30% of estimated new cases and 15% of deaths of female cancers in 2020 and poses severe threats to women's lives and health (1). Immune infiltration plays a pivotal role in regulating cancer progress and metastatic dissemination in this solid tumor. However, prognostic biomarkers to assess the tumor immune infiltration are still unavailable in breast cancer.

The transmembrane p24 trafficking protein (*TMED*) family contains 10 members (*TMED*1–10) involved in cargo protein transport in the secretory pathway. Among them, *TMED*2 has been shown to be more highly expressed in sphere-shaped clones of 4T1 murine breast cancer cells than in non-sphere-shaped clones (2). *TMED3* and *TMED9* have been found to exert pro-tumorigenic effects in human breast cancer (3,4). Meanwhile, the *TMED* family also have been reported to be involved in several other solid malignancies. The role of *TMED3* varies widely depending on the distinct tissue origins; it has been reported as a metastatic suppressor in human colon cancer but as an oncogene in hepatocellular carcinoma, renal cell carcinoma, and lung cancer (5-7). *TMED5* was shown to promote malignancy by interaction with *WNT7B* in cervical cancer (8). Higher *TMED9* expression was revealed to predict the poor clinical outcomes of patients in hepatocellular carcinoma and to facilitate colon cancer metastasis via the *CNIH4/TGFα/GLI* pathway (5,9). Overall, the *TMED* family members participate in the initiation and progression of numerous tumor types. In addition, aberrant expression of *TMED* proteins has been shown to cause morphological abnormalities and lead to a broad spectrum of diseases, especially in the dysregulation of immune responses. Loss of *TMED1* expression was shown to reduce the production of interleukin 33 (*IL-33*), which was reported to medicate intra-tumoral immunosuppression in breast cancer (10,11). *TMED7* was found to inhibit the immunoadjuvant toll-like receptor 4 (*TLR4*) pathway, which is essential for radiotherapy and chemotherapy (12,13). However, integrative analysis is still lacking to assess the clinical relevance of *TMED* family members in breast cancer. Still, their biological roles in the tumor immune microenvironment are currently poorly understood.

In the present study, we screened the prognostic factors of the *TMED* family in BC and explored their correlation with tumor-immune infiltration using bioinformatics tools. We also validated the expressions of these prognostic factors in human tissue samples and identified their cellular phenotypes and functional properties in breast cancer cell lines. In doing so, we sought to elucidate the diagnostic and prognostic value of the *TMED* family in breast cancer (14). We present the following article in accordance with the MDAR reporting checklist (available at https://atm.amegroups.com/article/view/10.21037/atm-22-5444/rc).

Methods

Gene expression analysis and ROC analysis

We downloaded five microarray datasets related to breast cancer from the public Gene Expression Omnibus (GEO) database (www.ncbi.nlm.nih.gov/geo/): GSE65212, GSE42568, GSE5364, GSE22820 and GSE45827. The RNA-seq data of invasive breast carcinoma (BRCA) based on 1,097 breast cancer samples and 113 normal breast tissues were acquired in the Genomic Data Commons (GDC) portal (http://portal.gdc.cancer.gov/) and calculated using R software version 4.0.3 (The R Foundation of Statistical Computing, Vienna, Austria). eDatasets above were analyzed using the "Bioinformatics analysis" module on the HOME-for-Researchers website (https://www.home-for-researchers.com/static/index.html#/) and Sangerbox software (http://www.sangerbox.com/tool). Receiver operating characteristic curve (ROC) analysis was performed using the statistic tool of the HOME-for-Researchers website.

The comparison of proteomic data between primary tumor and normal tissue in breast cancer was analyzed using the Clinical Proteomic Tumor Analysis Consortium (CPTAC) module of the University of ALabama at

Birmingham CANcer data analysis portal (UALCAN) database (http://ualcan.path.uab.edu/index.html) (15). A P value less than 0.05 was considered statistically significant.

Analyses of clinicopathologic variables and patient outcomes

Targeted expression analysis of the *TMED* family was conducted using the DNA microarray data of breast tumors and normal tissues from the Breast Cancer Gene-Expression Miner v4.8 (http://bcgenex.ico.unicancer.fr/BC-GEM/GEM-Accueil.php?js=1) (16). The receptor status, nodal status, histological status, Scarff-Bloom-Richardson score (SBR), Nottingham Prognostic Index (NPI) and age were explored. All P values smaller than 0.05 were considered statistically significant.

Kaplan-Meier survival curves were generated using the publicly available database Kaplan-Meier Plotter (KM-Plotter; http://kmplot.com/analysis/) (17). The breast cancer patients were split by the median levels of TMED family members, and the log-rank P values less than 0.05 were considered statistically significant.

Analysis of tumor immunity

We used the "Immune module" of the "Immune Association" part in the web tool Tumor IMmune Estimation Resource 2.0 (TIMER2.0; http://timer.comp-genomics.org/) to assess the associations between *TMED* expression and tumor-infiltrating immune cells in breast cancer (18). The correlations between *TMED* expression and landmark genes of immune cells were also evaluated by the "Gene_Corr module" of this website's "Cancer Exploration" part. The "Purity Adjustment" option was selected according to the website developer's recommendation. Filter criteria: P value less than 0.05 and $|\text{Rho ratio}| \geq 0.1$.

The relationship between key *TMED* members and the immune checkpoint genes was analyzed and visualized by the "Gene-Immune Analysis" module of SangerBox (http://sangerbox.com/).

A total of 2,483 immune-related genes were obtained from the "Shared Data" module of ImmPort database (https://www.immport.org/home) and then utilized to generate an intersection with the common co-expressed genes of *TMED*2/3/4/9 by Venn diagram. GeneMANIA software (https://genemania.org/) was queried with default parameters to visualize the protein-protein interaction (PPI) networks between *TMED*2/3/4/9 and their common co-expressed immune-related genes (19).

Exploration of gene regulatory network

Genomic Profiles of *TMED* for breast invasive carcinoma [The Cancer Genome Atlas (TCGA); PanCancer Atlas] cohort were generated by querying the "Oncoprint" and "survival analysis" module of cBioPortal database (http://www.cbioportal.org). The co-expressed genes of *TMED*2/3/4/9 were downloaded from the "Co-expression" module (Filter criteria: P value <0.05 and |Spearman's Correlation value| ≥0.1), and the common correlated genes of *TMED*2/3/4/9 were generated by the webtool Venn diagram (http://bioinformatics.psb.ugent.be/webtools/Venn/). The top 200 positively co-expressed genes of *TMED*2/3/4/9 were separately entered into the Metascape database (http://www.metascape.org) to perform Gene Ontology (GO) enrichment analysis (20), and their common positively co-expressed genes together with *TMED*2/3/4/9 were submitted into Expression2kinases (X2K) webtool to analyze the upstream regulators, including transcription factors and protein kinases enriched by known PPIs (https://maayanlab.cloud/X2K/) (21).

The multi-omics database LinkedOmics was queried for analyzing *TMED*-related microRNAs (miRNAs; http://www.linkedomics.org/login.php) (22). Specifically, the RNAseq data of BRCA from platform HiSeq RNA and the miRNASeq data from HS miR were chosen as the "Search dataset" and "Target dataset", respectively. *TMED* was submitted as the "Attribute" and Pearson Correlation test as the "Statistical Method". The Function module LinkFinder analyzed *TMED* associated miRNAs, and the results were downloaded. Then *TMED*2/3/4/9 and their commonly associated miRNAs were submitted into the Cytoscape software 3.8.2 (https://cytoscape.org/), and the interaction network was visualized based on their positive or negative correlations.

Human tissue samples and cell lines

This study was conducted in accordance with the principles stated in the Declaration of Helsinki (as revised in 2013). Ethical clearance was granted from the First Affiliated Hospital of Nanjing Medical University Medical Science Research Ethics Committee (Ethics code: 2021-SR-308). Breast cancer specimens were harvested from the Department of General Surgery, the First Affiliated

Hospital of Nanjing Medical University, and written informed consent was provided by the patients or their next of kin. Surgical specimens were resected, snap-frozen in liquid nitrogen, and deposited in the Biological Sample Bank of Jiangsu Province Hospital. The catalogue number of samples used in this study were 399, 459, 461, 474, 476, 477 and 488. The breast tumor cells MCF-7, ZR-75-1, BT-474, SK-BR-3, MDA-MB-453, MDA-MB-231, BT-549, Hs-578T, HCC1806, and HCC1937 were purchased from the Cell Bank of the Chinese Academy of Sciences (Shanghai, China). For western blot analysis, frozen human breast cancer samples were ground and homogenized in a mortar and pestle under liquid nitrogen and then lysed in radioimmunoprecipitation assay (RIPA) lysis buffer (Solarbio, Beijing, China) supplemented with protease inhibitors phenylmethylsulfonyl fluoride (PMSF; Beyotime, Shanghai, China). Cells were rinsed twice with phosphate-buffered saline (PBS) and lysed in RIPA buffer on ice.

Western blot assay

The lysates were mixed with 5× protein loading buffer (NCM Biotech, Suzhou, China) and denatured at 99 ℃ for 10 minutes. Equivalent amounts of total tissue or cellular proteins were separated on a 12.5% sodium dodecyl sulfate polyacrylamide gel electrophoresis (SDS-PAGE) gel and subsequently transferred onto polyvinylidene fluoride (PVDF) membranes (Millipore, USA) at constant 200 mA for 50 minutes. After blocking with 5% milk in tris-buffered saline with Tween 20 (TBST) for 6 hours at room temperature, the membranes were incubated with primary antibodies overnight at 4 ℃ and corresponding secondary antibodies at room temperature for 1 hour. Finally, membranes were rinsed 3 times in TBST, exposed with enhanced chemiluminescence (ECL) Plus (Yeasen Biotechnology, China), and imaged on Bio-Rad ChemDoc XRS (Bio-Rad, Hercules, CA, USA). Before re-blotting with another antibody, the membranes were stripped by incubating with weak stripping buffer (Beyotime, China) for 15 minutes and re-blocked for 6 hours. Antibodies used were as follows: anti-*TMED2* (1:500, Proteintech, Wuhan, China), anti-*TMED3* (1:500, Proteintech), anti-*TMED4* (1:300, Proteintech), anti-*TMED9* (1:500, Proteintech).

Cell culture and siRNA transfection

Most cells were cultured in basic medium with 10% fetal bovine serum (FBS; the specific culture conditions are listed in Table S1). One day before small interfering RNA (siRNA) transfection, cells were plated at 3×10^5 cells per well in a 6-well plate. Next day, the plated cells with about 30–50% confluence were washed, and fresh complete medium replaced before treatment. A total of 100 pmol of siRNA against *TMED2/3/4/9* or negative control siRNA (RiboBio, Guangzhou, China) were added into 125 μL Opti-MEM medium, complexed with 4ul lipofectamine 8000 (Beyotime).

The siRNA target sequences were as follows:

TMED2 siRNA, GGAAGTCCGGGAGAGAATA;

TMED3 siRNA, GTCAGGTGCTACTGTTGAA;

TMED4 siRNA, CTACCAGGATGGCTCTCTT;

TMED9 siRNA, GCTGCTAAAGACAAGTTGA.

The control sequence (siCONTROL non-targeting siRNA) was from RiboBio.

After resting for 20 minutes, the transfection mix was added dropwise to each well in the 6-well plate. The transfected cells were continually cultured for 48 hours before being harvested.

Wound healing and transwell invasion assay

For wound healing assays, a linear scratch was made on the single-cell layer using a pipette tip, and then the cells were incubated in a fresh medium containing 0.5% FBS for 48 hours. Images of the scratch wounds were captured using a phase-contrast microscope at 0, 24, and 48 hours after scratching, and wound areas were measured using the Image J software (National Institutes of Health, Bethesda, MD, USA).

Transwell invasion assay was carried out using the 24-well transwell chamber (Costar, Washington, DC, USA) with a pore size of 8 μm. Briefly, the Matrigel [Becton, Dickinson, and Co. (BD) Biosciences, Franklin lakes, NJ, USA] was diluted 1:9 with serum-free medium and added into the upper chamber in a 24-well plate. After matrix gel solidification, 1×10^5 cells were added into the chamber, embedded in the medium with 20% FBS immediately. After incubation for 24 hours, the invading cells on the basal side of the chambers were fixed with 4% paraformaldehyde (PFA), dyed with 0.1% crystal violet, and imaged using a Zeiss Axiocam camera (Zeiss, Oberkochen, Germany).

Statistics

The bioinformatics data of the *TMED* family were generated by the online web tools. The ROC curve was

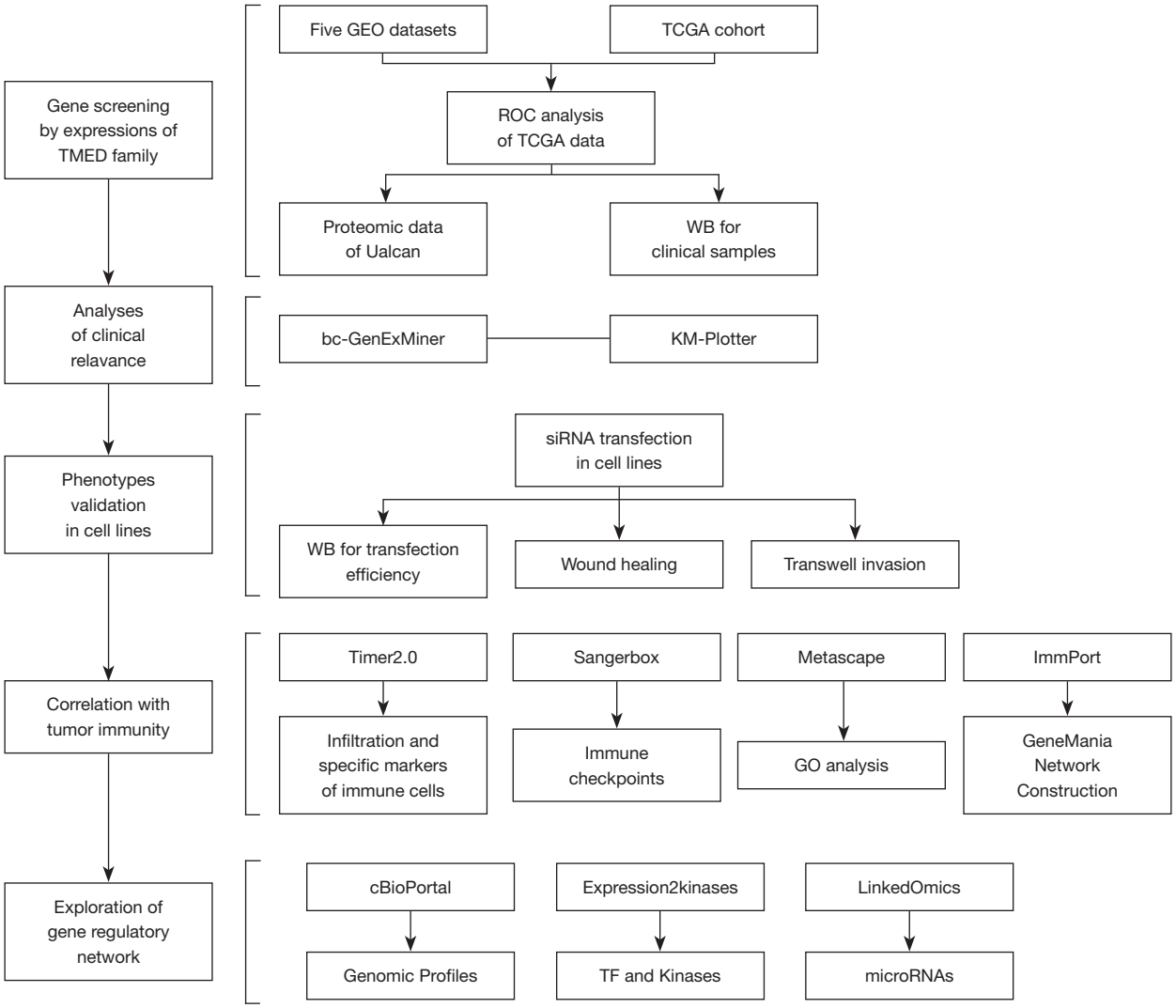

Figure 1 A flowchart of study design illustrating analytical and experimental procedures. GEO, Gene Expression Omnibus; TCGA, The Cancer Genome Atlas; siRNA, small interfering RNA; TMED, transmembrane p24 trafficking protein; ROC, receiver operating characteristic; WB, Western blotting; KM-Plotter, Kaplan-Meier Plotter; GO, Gene Ontology; TF, transcription factor.

calculated by the website based on R software version 4.0.3. Statistical analysis of cell migration and invasion data was conducted using paired or independent samples *t*-test. A P value less than 0.05 was considered statistically significant.

Results

TMED2/3/4/9 was highly expressed in breast cancer tissues and had the diagnostic potential to distinguish breast tumors from normal tissues

According to the study workflow (*Figure 1*), we first analyzed *TMED* messenger RNA (mRNA) levels in the 5 GEO microarray datasets of breast cancer, and found expression profiles of *TMED*2/3/4/9 were significantly elevated in tumors relative to normal tissues, whereas *TMED6* was remarkably reduced in cancer tissues. Similar results were obtained from the transcriptome data of TCGA BRCA cohort (*Figure 2A* and Figure S1). Thus, we selected *TMED*2/3/4/6/9 for further analysis because they showed a consistent trend of changes in both datatypes.

Then, we performed ROC analysis to determine the predictive values of *TMED*2/3/4/6/9 using mRNA

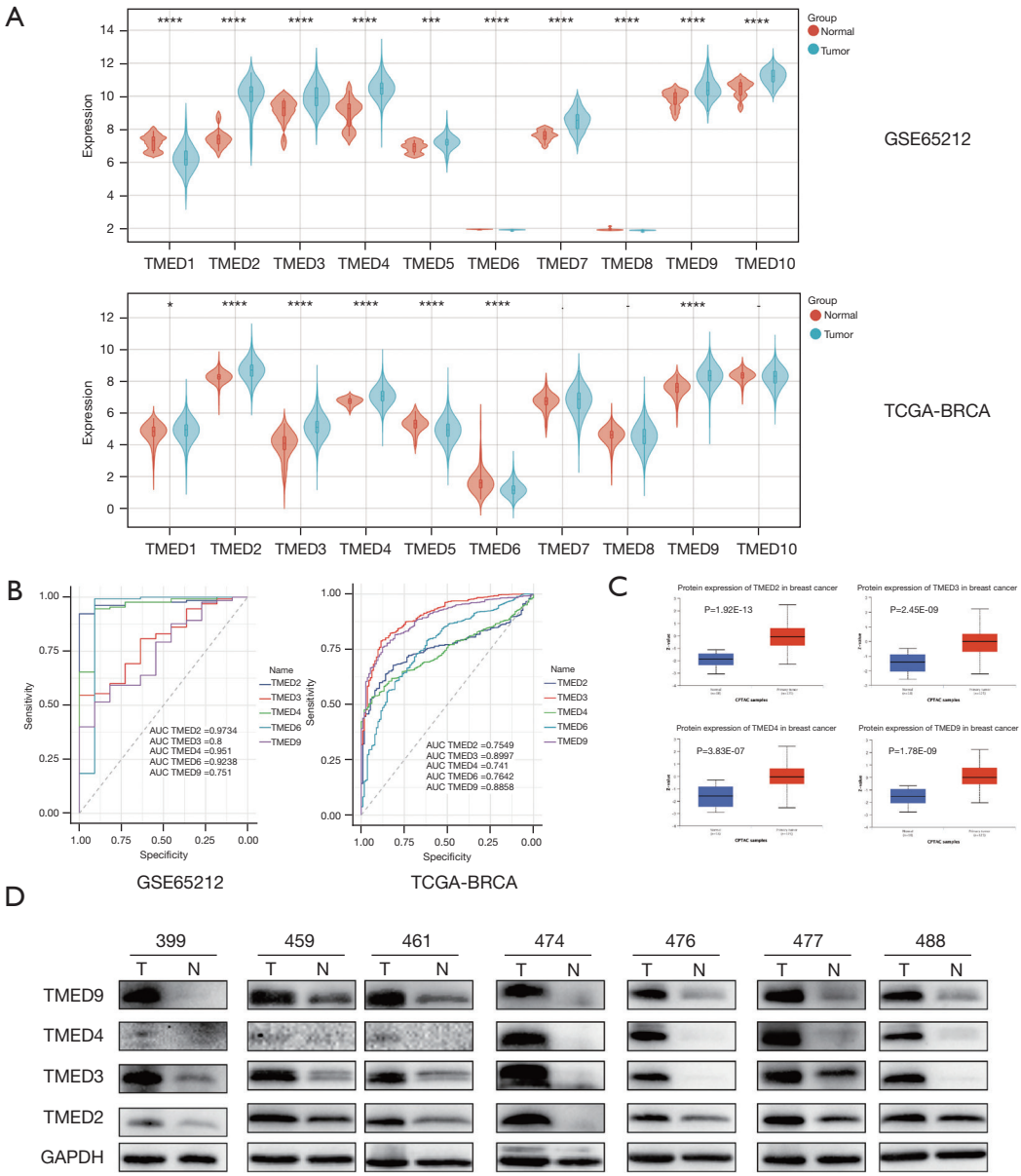

Figure 2 The expressions and diagnostic value of TMED2/3/4/9 in breast cancer tissues (A) Comparison of the expressions of TMED family in breast cancer tissue and normal tissue by analyzing the GEO microarray dataset GSE65212 as well as the RNA sequencing data from TCGA-BRCA cohort. TMED2/3/4/9 was upregulated, while TMED6 was downregulated in cancer tissues. Filter criteria: P value <0.05. (B) ROC curve analysis of candidate genes of TMED family based on their expressions in GSE65212 and TCGA-BRCA datasets. GSE65212 dataset: TMED2: AUC (95% CI), 0.9734 (0.9483, 0.9986); TMED3: AUC (95% CI), 0.8 (0.6872, 0.9128); TMED4: AUC (95% CI), 0.951 (0.889, 1); TMED6: AUC (95% CI), 0.9238 (0.7787, 1); TMED9: AUC (95% CI), 0.751 (0.6177, 0.8844); TCGA-BRCA dataset: TMED2: AUC (95% CI), 0.7549 (0.7227, 0.7871); TMED3: AUC (95% CI), 0.8997 (0.873, 0.9264); TMED4 AUC (95% CI), 0.741 (0.7088, 0.7732); TMED6 AUC (95% CI), 0.7642 (0.7199, 0.8086); TMED9 AUC (95% CI), 0.8858 (0.8602, 0.9114). (C) Analysis of TMED2/3/4/9 protein level, based on proteomic CPTAC data from UALCAN database. (D) TMED2/3/4/9 protein levels in paired cancerous and non-cancerous mammary samples identified by western blot assay. *, P<0.05; ***, P<0.001; ****, P<0.0001. TMED, transmembrane p24 trafficking protein; TCGA, Then Cancer Genome Atlas; BRAC, breast carcinoma; GEO, Gene Expression Omnibus; ROC, receiver operating characteristic; AUC, area under the curve; CPTAC, Clinical Proteomic Tumor Analysis Consortium; UALCAN, University of Alabama at Birmingham CANcer data analysis portal.

expression data of GSE65212 and TCGA BRCA cohort (*Figure 2B*), and found that the area under the ROC (AUC) for all candidate *TMED* members were more than 0.7, indicating that *TMED*2/3/4//6/9 could distinguish cancer samples from healthy controls {GSE65212 dataset: *TMED2*: AUC [95% confidence interval (CI)], 0.9734 (0.9483, 0.9986); *TMED3*: AUC (95% CI), 0.8 (0.6872, 0.9128); *TMED4*: AUC (95% CI), 0.951 (0.889, 1); *TMED6*: AUC (95% CI), 0.9238 (0.7787, 1); *TMED9*: AUC (95% CI), 0.751 (0.6177, 0.8844); TCGA-BRCA dataset: *TMED2*: AUC (95% CI), 0.7549 (0.7227, 0.7871); *TMED3*: AUC (95% CI), 0.8997 (0.873, 0.9264); *TMED4* AUC (95% CI), 0.741 (0.7088, 0.7732); *TMED6* AUC (95% CI), 0.7642 (0.7199, 0.8086); *TMED9* AUC (95% CI), 0.8858 (0.8602, 0.9114)}.

To validate the mRNA and protein concordance of candidate *TMED* members, we queried the proteomic CPTAC data from the UALCAN database (*TMED6* data was not available) and confirmed a significant increase in *TMED*2/3/4/9 protein levels in breast cancer (*Figure 2C*). Further, we assessed their protein levels in paired cancerous and non-cancerous mammary samples from 7 patients using western blot assay. As expected, higher protein levels of *TMED*2/3/4/9 were corroborated in most breast cancer tissues compared with paired adjacent normal tissues (*Figure 2D*).

The correlations between aberrantly expressed TMED2/3/4/9 and clinical variables as well as patient prognosis in breast cancer

To evaluate the clinical and pathological roles of *TMED*2/3/4/9 in breast cancer, we next performed correlation analysis of *TMED*2/3/4/9 expression levels with clinical parameters by bc-GenExMiner. Specifically, higher *TMED*3/4/9 expressions were observed in the >51-year age group than those in the ≤51-year age group. The expression of *TMED4* and *TMED9* were higher in lymph node-positive patients than lymph node-negative patients, suggesting their potential roles in local invasion and metastasis. Meanwhile, the expression of *TMED2* and *TMED9* was positively correlated with SBR and NPI, suggesting that high expression of *TMED2* and *TMED9* in poorly differentiated tumors at diagnosis might indicate an adverse prognosis (*Figure 3A*).

We then examined the differential expression of *TMED*2/3/4/9 in breast cancer stratified according to the protein level of estrogen receptor (ER), progesterone receptor (PR), human epidermal growth factor receptor-2 (HER-2), and the triple-negative breast cancer (TNBC) status. Briefly, *TMED*3/9 trended towards higher mRNA expressions in hormone receptor (HR)-negative tumors than HR-positive tumors. Instead, HR-positive tumors expressed relatively high levels of *TMED*4, respectively. In addition, relative expression of *TMED*2/3/9 was increased in HER-2 positive tumors compared with HER-2 negative tumors, whereas *TMED*4 showed an opposite trend. Notably, only *TMED9* mRNA level was enriched in TNBCs compared to non-TNBCs, whereas *TMED*2/3/4 displayed an opposite expression pattern (*Figure 3B*).

To verify the effect of the *TMED* family on patient survival, we performed Kaplan-Meier meta-analyses of recurrent-free survival (RFS) and overall survival (OS) using the mRNA chip data of breast cancer in the KM-Plotter database. We found that higher expression of *TMED*2/3/4/9 correlated with shorter RFS. Furthermore, breast cancer patients with elevated *TMED*2/9 mRNA levels had a significantly lower OS. In short, a higher mRNA level of *TMED*2/3/4/9 was correlated with a less favorable prognosis of breast cancer patients (*Figure 3C*).

Knockdown of TMED2/3/4/9 by siRNA transfection inhibited the migration and invasion of MDA-MB-231 and HCC1937 cells in vitro

To explore the impact of *TMED*2/3/4/9 on the phenotypes of breast cancer, we first examined the relative expressions of *TMED*2/3/4/9 in different breast cancer lines (*Figure 4A*), and further treated MDA-MB-231 and HCC1937 cells by transient transfection of siRNAs, respectively. We confirmed that the protein levels of *TMED*2/3/4/9 were remarkably suppressed by their corresponding siRNAs (*Figure 4B*). Next, we analyzed the impacts of transfection by wound-healing assay and found that the migration rates of tumor cells significantly decreased relative to the negative control in both cell lines (*Figure 4C*). Consistent with the above results, cells that traversed matrix gel and invaded into the lower chamber were remarkably reduced in the experimental group compared to the negative control (*Figure 4D*). Together, down-regulation of *TMED*2/3/4/9 suppressed the migratory and invasive abilities of breast cancer cells *in vitro*.

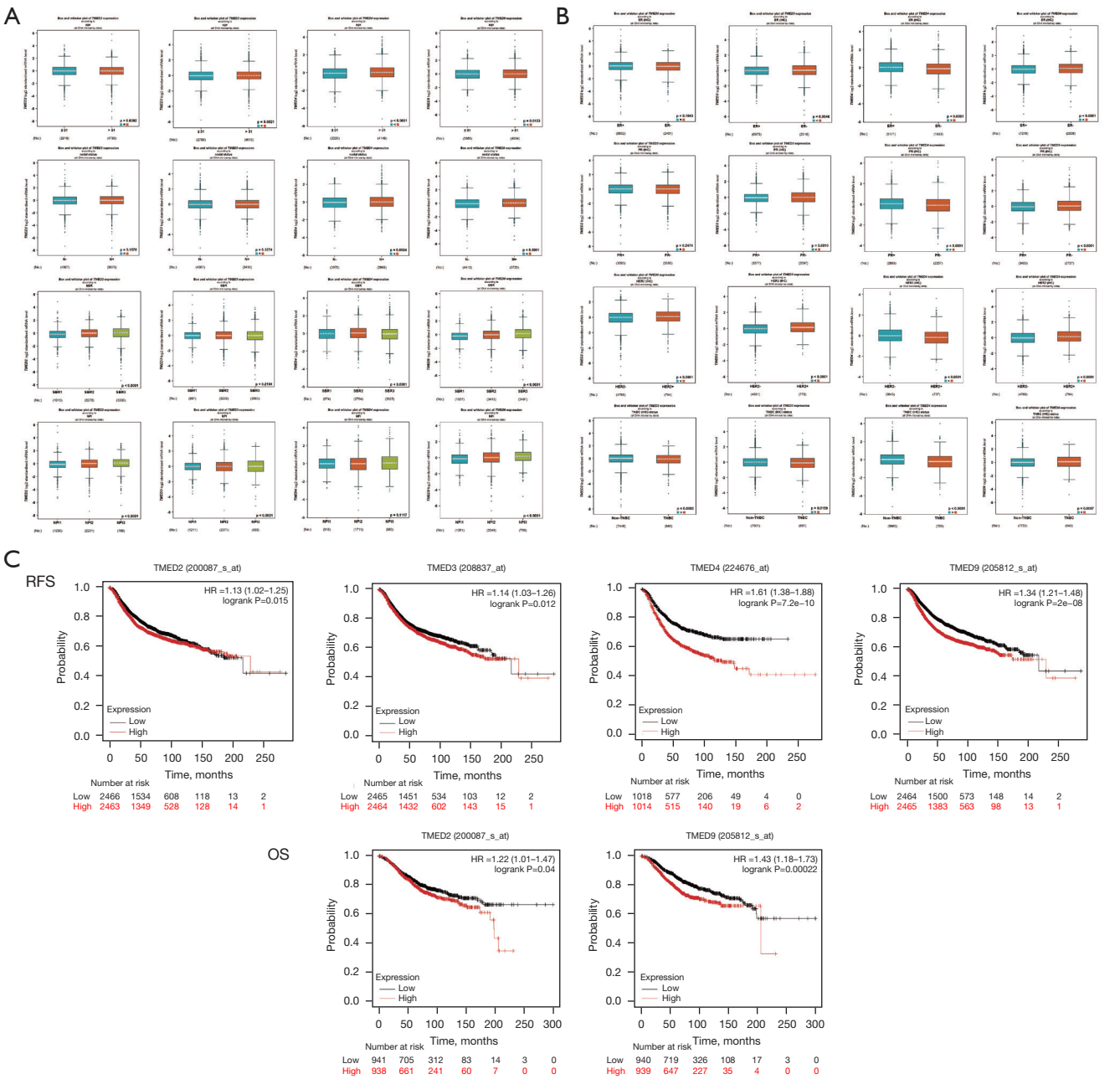

Figure 3 TMED2/3/4/9 expressions correlated with clinicopathological parameters and patient prognosis in breast cancer. (A) Breast cancer transcriptomic data were analyzed to correlate TMED2/3/4/9 expression with clinical and pathological features, including age, node status, SBR score, and NPI. (B) Comparison of TMED2/3/4/9 among different molecular subtypes of breast cancer. (C) Prognostic impact of TMED2/3/4/9 in breast cancer based on the mRNA gene chip data from the KM-Plotter database. TMED, transmembrane p24 trafficking protein; SBR, Scarff-Bloom-Richardson; NPI, Nottingham Prognostic Index; mRNA, messenger RNA; KM-Plotter, Kaplan-Meier Plotter; RFS, recurrent-free survival; OS, overall survival.

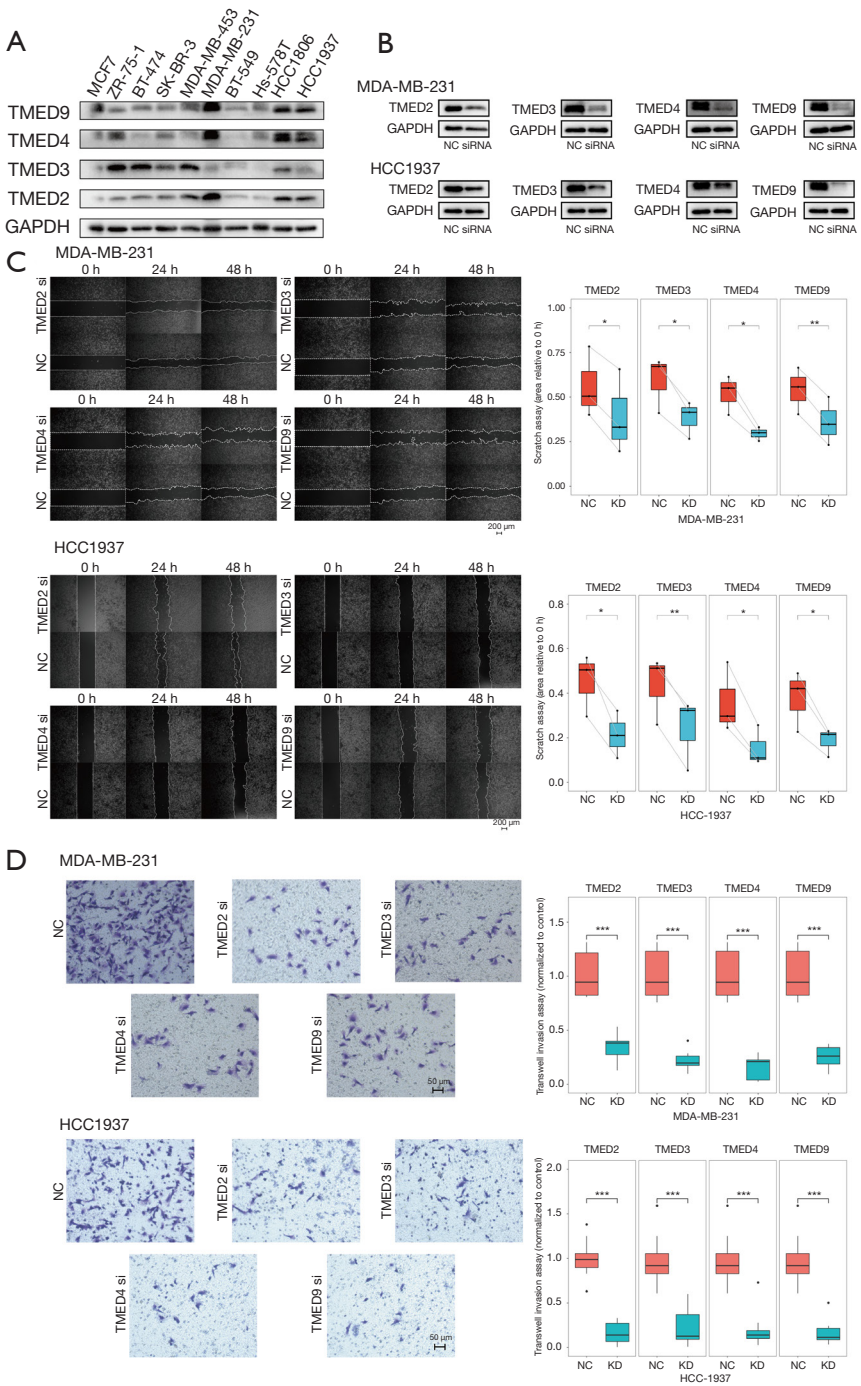

Figure 4 Knockdown of TMED2/3/4/9 remarkably inhibited the migration and invasion of breast cancer *in vitro*. (A) The relative expressions of TMED2/3/4/9 in different breast cancer lines (B) The efficiency of siRNA transfection was validated by western blot assay. The protein levels of TMED2/3/4/9 were remarkably down-regulated in both MDA-MB-231 and HCC1937 cell lines. (C) The migration capabilities of MDA-MB-231 and HCC1937 cells after siRNA transfection were determined by wound healing assay. (D) Cell migration abilities of MDA-MB-231 and HCC1937 cells transfected siRNAs were evaluated by transwell invasion assays. The invading cells on the basal side of the chambers were dyed with 0.1% crystal violet. Each experiment was repeated at least 3 times independently with the similar results. *, P<0.05; **, P<0.01; ***, P<0.001. TMED, transmembrane p24 trafficking protein; GAPDH, glyceraldehyde-3-phosphate dehydrogenase; siRNA, small interfering RNA; NC, negative control group; KD, knockdown group.

High expressions of TMED2/3/4/9 played essential roles in tumor immunity and indicated the immunosuppressive status in breast cancer.

We queried the TIMER2.0 database to infer immune component abundance depending on the expression of *TMED*2/3/4/9 in breast cancer (*Table 1*). Based on most of the algorithms, there was an inverse correlation between their mRNA levels and the infiltration of tumor-suppressive immune cells, including *TMED*3/9 and $CD8^+$ T cells, *TMED*2/3/4 and T follicular helper cells, *TMED*3/4 and dendritic cells (DCs), as well as *TMED*2/3/4 and natural killer (NK) cells. We also observed the positive associations between *TMED*3/4 levels and M2-type macrophages infiltrates as well as their negative correlation with M1-type macrophages. However, *TMED*2/9 was positively correlated with both types of macrophages.

Afterward, we analyzed the associations between *TMED*2/3/4/9 expression and landmark genes of immune cells. As shown in *Table 2*, *TMED*2/3/4 was inversely related to hallmarks of 2 major adaptive immune cells, including general T cells (*CD3D*, *CD3E*, *CD2*) and B cells (*CD19*, *CD79A*). Consistent with the above immune cell types estimated by multiple algorithms, *TMED3* was inversely associated with $CD8^+$ T cells (*CD8A*, *CD8B*) and DCs, whereas *TMED*3/4 was negatively correlated with NK cells. In addition, *TMED*2/9 positively correlated with specific markers of M2-type macrophages (*CD163*, *MS4A4A*, and *VSIG4*) and tumor-associated macrophages (*CCL-2*, *CD68*, *IL10*).

For the relationship between *TMED*2/3/4/9 and the immune checkpoint genes, we noted that *TMED*2/3/4/9 showed negative correlations with a range of immune checkpoint genes such as *PD-1* and *CTLA4*, which might indicate the immunosuppressive status in breast cancer (*Figure 5A*).

Based on GO enrichment analysis of the top 200 co-expressed genes of TMED2/3/4/9, we found that each member of TMED2/3/4/9 participated in the immune system process (*Figure 5B*). We also identified *CCR6*, *TXK*, *TSLP*, *BACH2*, and *PTGFR* as the common co-expressed immune-related genes of *TMED*2/3/4/9, their prognostic values in breast cancer (Figures S2,S3 and Tables S2-S4) and the interactome network generated by GeneMANIA elucidated their central roles in the gene regulatory network (*Figure 5C*).

Exploration of genomic profiles, upstream regulators, and related miRNAs of TMED2/3/4/9

To investigate genetic alterations of *TMED*2/3/4/9 in breast cancer samples, we focused on the genomic profiles of *TMED*2/3/4/9 in the selected TCGA PanCancer Atlas breast cancer cohort. The genetic alteration percent of *TMED*2/3/4/9 in 994 samples was 7%, 5%, 10%, and 9%, respectively, and their variability was dominated by high expressions of mRNA (*Figure 6A*). Further survival analysis indicated that the patients in the altered group had shorter progression free survival (PFS), OS, and disease free survival (DFS) compared to patients in the unaltered group (*Figure 6B*).

To probe the upstream regulatory network, we performed kinases and transcription factors enrichment analysis by submitting *TMED*2/3/4/9 and their common 54 positively correlated genes to X2K. As shown in *Figure 6C*, *TAF1*, *NFYB*, *NFYA*, *YY1*, *ZMIZ1*, *ERG*, *PML*, *SP2*, *IRF3*, and *SP1* were identified as the top 10 transcription factors, and *MAPK14*, *CDK1*, *MAPK1*, *CSNK2A1*, *CK2ALPHA*, *CDK4*, *MAPK3*, *MAPK8*, *GSK3B*, and *CDC2* as the top 10 protein kinases.

Given the importance of miRNAs in post-transcriptional regulation, we explored *TMED*2/3/4/9 associated miRNAs in breast cancer by extracting the data from LinkedOmics. Firstly, *TMED*2/3/4/9 correlated miRNAs were acquired, respectively, and then their common miRNAs were determined by further overlapping (Figure S4). As shown in the interaction network visualized by Cytoscape (*Figure 6D*), *TMED*2/3/4/9 shared the common related miRNAs including hsa-mir-1258, hsa-mir-125a, hsa-mir-1296, hsa-mir-142, hsa-mir-204, hsa-mir-20a, hsa-mir-296, hsa-mir-326, hsa-mir-328, hsa-mir-331, hsa-mir-550a-1, hsa-mir-550a-2, hsa-mir-628, hsa-mir-7-1, hsa-mir-744, and hsa-mir-99b. Among them, only hsa-mir-1258 and hsa-mir-204 negatively correlated with all of the 4 members, whereas the other miRNAs positively related to some *TMED*s only occasionally. In brief, aberrant expression of *TMED*2/3/4/9 was determined at the gene level and transcriptional level and interacted with a seizes of epigenetic regulators such as miRNAs.

Discussion

The *TMED* family members serve as important regulators

Table 1 Analysis of the association between the mRNA levels of TMED2/3/4/9 and immune cell infiltration in breast cancer by TIMER2.0 database

Immune cells	Algorithms	TMED2	TMED3	TMED4	TMED9
T cell CD8$^+$	TIMER	0.233*	0.08	0.146*	−0.024
	EPIC	0.214*	−0.075	0.237*	−0.112#
	MCPCOUNTER	−0.098	−0.152#	−0.084	−0.031
	CIBERSORT	−0.187#	−0.101#	−0.141#	−0.071
	CIBERSORT−ABS	−0.121#	−0.162#	−0.089	−0.047
	QUANTISEQ	−0.052	−0.17#	−0.058	−0.037
	XCELL	−0.012	−0.174#	−0.039	−0.068
Subtype	Naive_XCEL	−0.007	−0.229#	−0.073	−0.14#
	Central memory_XCEL	0.024	−0.154#	−0.055	−0.065
	Effector memory_XCELL	−0.124#	−0.109#	−0.1	−0.03
T cell follicular helper	CIBERSORT	−0.227#	−0.137#	−0.216#	−0.047
	CIBERSORT−ABS	−0.133#	−0.203#	−0.13#	−0.019
DC cells	Myeloid dendritic cell_TIMER	−0.173#	−0.066	−0.093	0.13*
	Myeloid dendritic cell_XCELL	−0.045	−0.151#	−0.152#	0.015
	Myeloid dendritic cell_MCPCOUNTER	0.004	−0.182#	0.039	−0.103#
	Myeloid dendritic cell_QUANTISEQ	0.207*	−0.08	0.097	−0.081
	Myeloid dendritic cell activated_XCELL	−0.111#	−0.135#	−0.187#	0.044
	Plasmacytoid dendritic cell_XCELL	−0.012	−0.069	−0.179#	0.07
NK cells	NK cell_EPIC	−0.247#	−0.062	−0.355#	0.121*
	NK cell_MCPCOUNTER	0.017	−0.238#	0.01	−0.066
	NK cell_QUANTISEQ	−0.148#	−0.181#	0.051	−0.102#
	NK cell_XCELL	0.051	0.004	0.053	0.06
	NK cell activated_CIBERSORT	−0.221#	−0.062	−0.198#	0.001
	NK cell activated_CIBERSORT−ABS	−0.199#	−0.109#	−0.175#	0.02
Macrophage	EPIC	−0.061	−0.075	−0.129#	0.172*
	TIMER	0.317*	0.101*	0.222*	0.098
	XCELL	0.095	0.045	−0.076	0.208*
	M0_CIBERSORT	−0.04	0.032	−0.108#	0.148*
	M0_CIBERSORT−ABS	−0.035	−0.033	−0.106#	0.148*
	M1_CIBERSORT	0.128*	−0.112#	−0.064	−0.015
	M1_CIBERSORT−ABS	0.093	−0.164#	−0.025	−0.002
	M1_QUANTISEQ	0.139*	0.055	−0.007	0.124*
	M1_XCELL	−0.037	0.012	−0.189#	0.242*
	M2_CIBERSORT	0.187*	0.189*	0.172*	0.139*

Table 1 (*continued*)

Table 1 (*continued*)

Immune cells	Algorithms	TMED2	TMED3	TMED4	TMED9
	M2_CIBERSORT–ABS	0.186*	–0.034	0.155*	0.114*
	M2_QUANTISEQ	0.078	0.022	0.178*	–0.023
	M2_XCELL	0.039	0.118*	–0.07	0.189*
	M2_TIDE	–0.116#	0.097	0.03	–0.086
	Macrophage/Monocyte_MCPCOUNTER	0.122*	–0.088	–0.017	0.109*

*, represents positive correlation (P<0.05 and Rho >0.1); whereas #, represents negative correlation (P<0.05 and Rho <–0.1). The regular numbers with colorless background indicate not significant. mRNA, messenger RNA; TMED, transmembrane p24 trafficking protein; DC, dendritic cells; NK, natural killer.

of the vesicular trafficking of proteins in the cytoplasm. They mainly participate in the anterograde transport of coatomer II (COP II) coated vesicles as well as the retrograde transport of coatomer I (COP I) coated vesicles between the endoplasmic reticulum and Golgi apparatus. *TMED7* could also aid the delivery of TLR4 to the plasma membrane (23). Additionally, *TMED10* forms a protein channel in the endoplasmic reticulum to facilitate the entry of cytosolic proteins lacking signal peptides by an unconventional protein secretion (24). It has been shown that dysregulation of *TMED* family members leads to morphological defects of the mouse embryo and participated in Alzheimer's disease, Mucin 1 kidney disease, and tumors in humans (25-27). Previous studies have revealed that the *TMED* family proteins influence the malignant progression of several cancers, including the pro-tumor effects of *TMED2*, *TMED3*, and *TMED9* on breast cancer, but it has remained unclear whether they could be used as ideal biomarkers for this tumor type. Increasing evidence has suggested that the tumor microenvironment has an important impact on the invasion and metastasis of solid tumors. To date, reports of *TMED* members on tumor immune infiltration have remained unavailable. Hence, we aimed to probe the roles of the whole *TMED* family in breast cancer, particularly their modulations on tumor immune responses. In this study, we observed that *TMED2/3/4/9* was highly expressed in breast cancer tissues at both mRNA and protein levels. We verified the high expression of *TMED2/3/9* in paired human breast cancer samples which were consistent with the previous studies (2-4). To our knowledge, our findings regarding the high expression of *TMED4* in breast cancer have not been previously reported. We also showed the diagnostic value of *TMED2/3/4/9* mRNA levels by ROC and the coincidence of their expression patterns at the protein level.

Previously, little attention has been paid to the histopathological importance of *TMED2/3/4/9* in breast cancer. However, we found that upregulated *TMED2/3/4/9* mRNA levels correlated a range of pathological parameters, which might explain the inverse associations between *TMED2/3/4/9* expression and patient survival. For example, higher levels of *TMED4/9* were observed in node-positive groups and increased *TMED2/9* expressions in high-grade tumors. We also found that *TMED2/3/4/9* levels varied enormously among different molecular subtypes in breast cancer. It might confirm that a high degree of tumoral heterogeneity had a considerable impact on the expression pattern of *TMED2/3/4/9* in this tumor. Noticeably, despite the positive correlation between *TMED3* mRNA level and HR status consistent with previous studies, its positive relation to HER-2 status contradicted Zhang *et al.*'s observations in tissue microarray (28). Moreover, the negative relation between *TMED3* mRNA level and TNBC status was not observed in Pei *et al.*'s study (3). These inconsistencies might be attributed to the variance of specimen types and sample size, for the data analyzed in this study were gene expression data from DNA microarrays of 11,359 samples which was quite different from previous formalin-fixed paraffin-embedded (FFPE) tissue samples. For the impacts of *TMED2/3/4/9* on the phenotypes of breast cancer cells, we observed that downregulation of their protein levels attenuated the migratory and invasive capacities of tumor cells *in vitro*. Consistent results were obtained in previous studies on *TMED3* and *TMED9* in breast cancer, and we observed similar effects of *TMED2* and *TMED4*, which had never been reported before. The oncologic roles of *TMED2/3/9* were also supported by similar results from the research on other tumors, including

Table 2 Correlation analysis of TMED2/3/4/9 mRNA levels and gene markers of immune cells in breast cancer

Immune cells	Gene markers	TMED2	TMED3	TMED4	TMED9
T cell (general)	*CD3D*	–0.113#	–0.195#	–0.161#	–0.009
	CD3E	–0.053	–0.207#	–0.102#	–0.052
	CD2	0.001	–0.201#	–0.081	–0.028
CD8+ T cell	*CD8A*	0.008	–0.206#	–0.013	–0.075
	CD8B	–0.098	–0.152#	–0.084	–0.031
Tex	*PD-1 (PDCD1)*	–0.173#	–0.19#	–0.126#	0.058
	CTLA4	–0.024	–0.203#	–0.139#	0.019
	LAG3	–0.128#	–0.17#	–0.201#	0.089
	TIM-3 (HAVCR2)	0.186*	–0.061	0.042	0.137*
	GZMB	–0.058	–0.166#	–0.209#	0.039
B cell	*CD19*	–0.132#	–0.143#	–0.106#	–0.048
	CD79A	–0.101#	–0.149#	–0.109#	–0.073
NK cell	*KIR2DL3*	0.031	–0.12#	–0.054	–0.017
	KIR2DL4	0.014	–0.134#	–0.083	0.002
	KIR3DL1	0.002	–0.115#	–0.043	0.016
	KIR3DL2	–0.027	–0.135#	–0.109#	–0.041
	KIR2DS4	0.029	–0.113#	–0.063	–0.033
DC	*HLA-DPB1*	–0.193#	–0.064	–0.096	0.119*
	HLA-DQB1	–0.113#	–0.118#	–0.132#	0.089
	HLA-DRA	0.049	–0.11#	–0.015	0.037
	BCDA-1 (CD1C)	–0.109#	–0.111#	0.015	–0.121#
	BDCA-4 (NRP1)	0.235*	–0.019	0.182*	–0.065
TAM	*CCL2*	0.043	–0.128#	–0.101#	0.002
	CD68	0.149*	–0.036	0.029	0.192*
	IL10	0.197*	–0.093	0.016	0.162*
M1 macrophage	*IRF5*	0.056	–0.05	0.15*	0.18*
	COX2 (PTGS2)	0.044	–0.142#	–0.012	–0.098
M2 macrophage	*CD163*	0.202*	–0.075	0.113*	0.199*
	VSIG4	0.092	–0.031	0.072	0.133*
	MS4A4A	0.17*	–0.085	0.056	0.118*

*, represents positive correlation (P<0.05 and Rho >0.1); whereas #, represents negative correlation (P<0.05 and Rho <–0.1). The regular numbers with colorless background indicate not significant. TMED, transmembrane p24 trafficking protein; mRNA, messenger RNA; DC, dendritic cells; NK, natural killer; TAM, tumor associated macrophages.

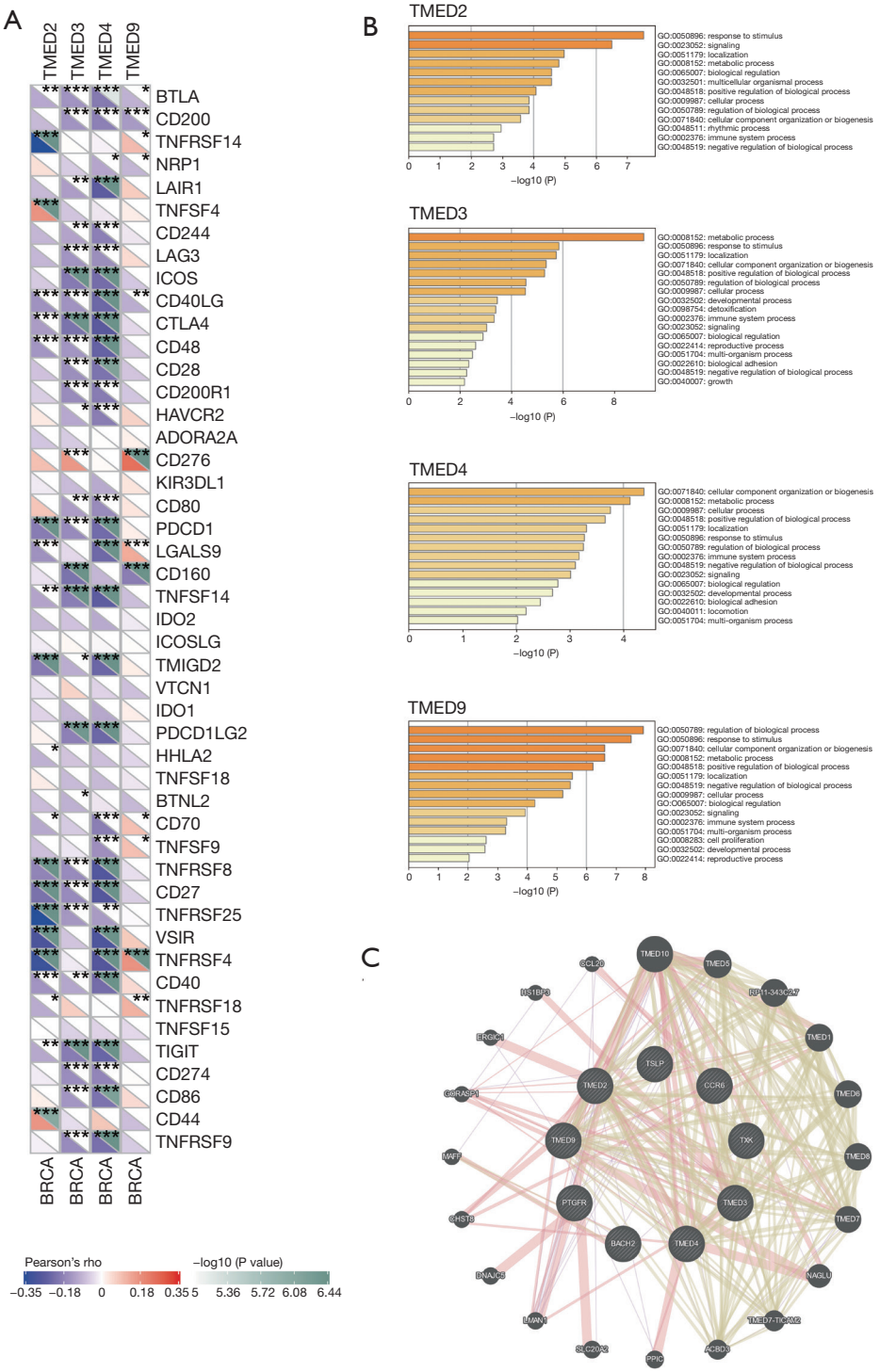

Figure 5 High expression of TMED2/3/4/9 indicated the immune-suppressive status in breast cancer. (A) Analysis of the relationship between the expressions of immune checkpoint genes and TMED2/3/4/9 mRNA levels was performed by the Sangerbox webtool. (B) GO enrichment analysis of the top 200 co-expressed genes of TMED2/3/4/9 generated by Metascape. (C) The interactome network of TMED2/3/4/9 and their common immune-related genes predicted by GeneMANIA database. *, P<0.05; **, P<0.01; ***, P<0.001. TMED, transmembrane p24 trafficking protein; BRCA, breast carcinoma; mRNA, messenger RNA; GO, Gene Ontology.

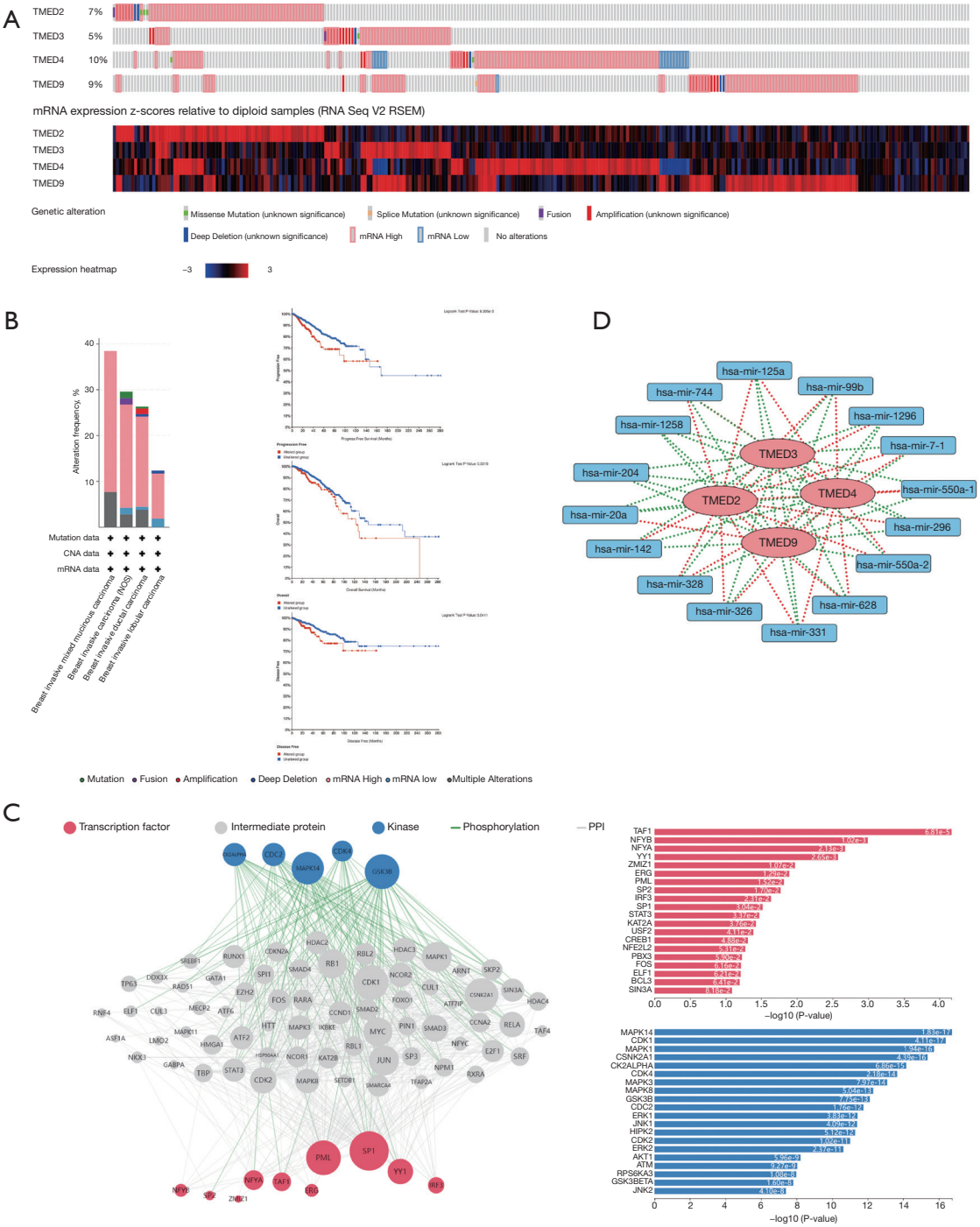

Figure 6 Gene regulatory network of TMED2/3/4/9 in breast cancer. (A,B) Genome alterations of TMED2/3/4/9 in breast cancer assessed by cBioportal database and the survival analysis between the altered and unaltered groups. (C) Upstream regulatory network of TMED2/3/4/9 and their common positively correlated genes was probed using Expression2kinases web tool, and the top transcription factors and protein kinases were displayed. (D) TMED2/3/4/9 and their co-associated miRNAs in breast cancer were extracted from LinkedOmics, and the network was generated by the software Cytoscape. TMED, transmembrane p24 trafficking protein; miRNA, microRNA; CNA, copy-number alteration; PPI, protein-protein interaction.

hepatocellular carcinoma, ovarian cancer, lung cancer, and chordoma (6,7,9,29-31). Interestingly, the opposed function of *TMED*9 against the metastatic suppressor effect of *TMED*3 in colon cancer might be caused by the distinct roles of the same gene based on the different genetic background (5).

Treatment for high-risk early TNBC with pembrolizumab has been determined to be a promising approach. The Food and Drug Administration (FDA) has approved it for use as (neo)adjuvant therapy for patients with this disease (32). Immune checkpoint inhibitor (ICB) responses are greatly influenced by the tumor microenvironment. Cells of the lymphoid and myeloid types make up the immune microenvironment of breast cancer. The lymphocytes in the body include $CD8^+$ T cells, $CD4^+$ T cells, T regulatory cells, B cells, and $CD38^+$ lymphocytes, while myeloid cells are mainly composed of macrophages, granulocytes, and dendritic cells (33). $CD8^+$ T cells and NK cells were more abundant in tumors that responded to PD-1 inhibitors than in nonresponsive tumors, and macrophages were less abundant (34). Additionally, tumors sensitive to ICB had an increased number of B cells and tertiary lymphoid structures (35). In spite of this, the role of the tumor microenvironment in modulating immune checkpoint inhibitor responses is still unclear. Therefore, identifying immunotherapy targets and biomarkers is critical to improving the effectiveness of therapy (36).

Although the requirement of *TMED*1 for innate immune signaling and the potentiating effects of *TMED*2 on anti-virus immunity, the roles of the *TMED* family on tumor immunity have not yet been clarified (11,37). Thus, we conducted multi-dimensional analysis on the *TMED* family, including their correlations with infiltrated immune cells and immune-cell specific markers. Importantly, our findings revealed that *TMED*2/3/4/9 could serve as potential biomarkers indicative of the immunosuppressive state in breast cancer, for their relative abundance inversely correlated with the infiltration of tumor antigen-presenting cells such as DCs and T follicular helper cells, and the tumor-killing effector cells including M1-type macrophages, $CD8^+$ T cells, and NK cells (38-44). Meanwhile, *TMED*3/4 expression was positively related to M2-type macrophages, which significantly contributed to tumor invasion, metastasis, and immune escape (45). Paradoxically, *TMED*2/9 was positively correlated with both types of macrophages but was only positively related to specific markers of M2-type macrophages. This discordance might be due to 2 different analytical approaches, and we tended to believe their combined results, that is, the positive correlation between *TMED*2/9 and M2-type macrophages rather than M1-type macrophages. Notably, *TMED*2/3/4/9 potentially emerged as a novel indicator in the field of immunotherapy for their negative correlations with numerous immune checkpoint genes, including the well-known *PD-1* and *CTLA4* (46,47). For the low response rates of breast cancer to immunotherapy, biomarkers like TMED2/3/4/9 that could distinguish immune-active or immune-suppressive status at the tumor site were helpful to identify the targeted population who might benefit from immunotherapy (48,49). Furthermore, we found that the co-expressed genes of *TMED*2/3/4/9 were enriched into the immune-related pathway, suggesting the important roles of *TMED*2/3/4/9 in tumor immunity.

We also investigated the potential underlying mechanisms of abnormal *TMED*2/3/4/9 expression at the genomic and transcriptional level as well as post-transcriptional level. Our findings suggested that genetic alterations of *TMED*2/3/4/9 had a considerable impact on patient survival, and their aberrant expression might be the integrated regulation effect of numerous kinases, transcription factors, and miRNAs. Interestingly, their common negatively correlated hsa-mir-1258 and hsa-mir-204 were tumor suppressors regulating the metastasis or immune microenvironment remodeling in breast cancer (50,51).

There were some shortcomings in the current study. First, due to the insufficient sample size for protein-level validation, more clinical samples should be collected to evaluate *TMED*2/3/4/9 expressions by different assays, including western blot and immunohistochemistry (IHC) staining. Importantly, to stratify patients with breast cancer, the correlations between IHC scores of TMED2/3/4/9 in tissues with other pathological parameters will help to find out the best cutoff value to predict the patients' outcomes. Second, the present works on *TMED*2/3/4/9's impact on tumor immunity and regulatory network were predominantly based on bioinformatic analysis. More experiments are needed to unravel the complex underlying mechanisms.

Conclusions

In summary, we conducted an integrative analysis of the roles of the *TMED* family in breast cancer by bioinformatic data-mining and experimental validation. We identified *TMED*2/3/4/9 as the potential immune-suppressive biomarkers in this tumor. Further study should focus on

confirming our findings by larger sample-sized specimens at the protein level, and the precise mechanism of their relationships with different types of immune-suppressive cells need to be elucidated.

Acknowledgments

The authors would like to gratefully acknowledge all of the patients and their families who contributed specimens to the study, and the surgical staff who assisted in the collection of specimens.

Funding: This research was supported by National Natural Science Foundation of China (No. 81902987); National Natural Science Foundation of China under Grant (No. 81872365); and the Jiangsu Province Postgraduate Cultivation Innovation Project-Graduate Research and Practice Innovation Program (No. KYCX21 1713).

Footnote

Reporting Checklist: The authors have completed the MDAR reporting checklist. Available at https://atm.amegroups.com/article/view/10.21037/atm-22-5444/rc

Data Sharing Statement: Available at https://atm.amegroups.com/article/view/10.21037/atm-22-5444/dss

Conflicts of Interest: All authors have completed the ICMJE uniform disclosure form (available at https://atm.amegroups.com/article/view/10.21037/atm-22-5444/coif). The authors have no conflicts of interest to declare.

Ethical Statement: The authors are accountable for all aspects of the work in ensuring that questions related to the accuracy or integrity of any part of the work are appropriately investigated and resolved. This study was conducted in accordance with the principles stated in the Declaration of Helsinki (as revised in 2013). Ethical clearance was granted from the First Affiliated Hospital of Nanjing Medical University Medical Science Research Ethics Committee (Ethics code: 2021-SR-308). Written informed consent was provided by the patients or their next of kin.

References

1. Siegel RL, Miller KD, Jemal A. Cancer statistics, 2020. CA Cancer J Clin 2020;70:7-30.
2. Lin X, Liu J, Hu SF, et al. Increased expression of TMED2 is an unfavorable prognostic factor in patients with breast cancer. Cancer Manag Res 2019;11:2203-14.
3. Pei J, Zhang J, Yang X, et al. TMED3 promotes cell proliferation and motility in breast cancer and is negatively modulated by miR-188-3p. Cancer Cell Int 2019;19:75.
4. Ju G, Xu C, Zeng K, et al. High expression of transmembrane P24 trafficking protein 9 predicts poor prognosis in breast carcinoma. Bioengineered 2021;12:8965-79.
5. Mishra S, Bernal C, Silvano M, et al. The protein secretion modulator TMED9 drives CNIH4/TGFα/GLI signaling opposing TMED3-WNT-TCF to promote colon cancer metastases. Oncogene 2019;38:5817-37.
6. Zheng H, Yang Y, Han J, et al. TMED3 promotes hepatocellular carcinoma progression via IL-11/STAT3 signaling. Sci Rep 2016;6:37070.
7. Xie A, Xu X, Kuang P, et al. TMED3 promotes the progression and development of lung squamous cell carcinoma by regulating EZR. Cell Death Dis 2021;12:804.
8. Yang Z, Sun Q, Guo J, et al. GRSF1-mediated MIR-G-1 promotes malignant behavior and nuclear autophagy by directly upregulating TMED5 and LMNB1 in cervical cancer cells. Autophagy 2019;15:668-85.
9. Yang YC, Chien MH, Lai TC, et al. Proteomics-based identification of TMED9 is linked to vascular invasion and poor prognoses in patients with hepatocellular carcinoma. J Biomed Sci 2021;28:29.
10. Jovanovic IP, Pejnovic NN, Radosavljevic GD, et al. Interleukin-33/ST2 axis promotes breast cancer growth and metastases by facilitating intratumoral accumulation of immunosuppressive and innate lymphoid cells. Int J Cancer 2014;134:1669-82.
11. Connolly DJ, O'Neill LA, McGettrick AF. The GOLD domain-containing protein TMED1 is involved in interleukin-33 signaling. J Biol Chem 2013;288:5616-23.
12. Doyle SL, Husebye H, Connolly DJ, et al. The GOLD

domain-containing protein TMED7 inhibits TLR4 signalling from the endosome upon LPS stimulation. Nat Commun 2012;3:707.
13. Apetoh L, Ghiringhelli F, Tesniere A, et al. Toll-like receptor 4-dependent contribution of the immune system to anticancer chemotherapy and radiotherapy. Nat Med 2007;13:1050-9.
14. Aber R, Chan W, Mugisha S, et al. Transmembrane emp24 domain proteins in development and disease. Genet Res (Camb) 2019;101:e14.
15. Chandrashekar DS, Bashel B, Balasubramanya SAH, et al. UALCAN: A Portal for Facilitating Tumor Subgroup Gene Expression and Survival Analyses. Neoplasia 2017;19:649-58.
16. Jézéquel P, Gouraud W, Ben Azzouz F, et al. bc-GenExMiner 4.5: new mining module computes breast cancer differential gene expression analyses. Database (Oxford) 2021;2021:baab007.
17. Győrffy B. Survival analysis across the entire transcriptome identifies biomarkers with the highest prognostic power in breast cancer. Comput Struct Biotechnol J 2021;19:4101-9.
18. Li T, Fu J, Zeng Z, et al. TIMER2.0 for analysis of tumor-infiltrating immune cells. Nucleic Acids Res 2020;48:W509-14.
19. Warde-Farley D, Donaldson SL, Comes O, et al. The GeneMANIA prediction server: biological network integration for gene prioritization and predicting gene function. Nucleic Acids Res 2010;38:W214-20.
20. Zhou Y, Zhou B, Pache L, et al. Metascape provides a biologist-oriented resource for the analysis of systems-level datasets. Nat Commun 2019;10:1523.
21. Clarke DJB, Kuleshov MV, Schilder BM, et al. eXpression2Kinases (X2K) Web: linking expression signatures to upstream cell signaling networks. Nucleic Acids Res 2018;46:W171-9.
22. Vasaikar SV, Straub P, Wang J, et al. LinkedOmics: analyzing multi-omics data within and across 32 cancer types. Nucleic Acids Res 2018;46:D956-63.
23. Liaunardy-Jopeace A, Bryant CE, Gay NJ. The COP II adaptor protein TMED7 is required to initiate and mediate the delivery of TLR4 to the plasma membrane. Sci Signal 2014;7:ra70.
24. Zhang M, Liu L, Lin X, et al. A Translocation Pathway for Vesicle-Mediated Unconventional Protein Secretion. Cell 2020;181:637-652.e15.
25. Jerome-Majewska LA, Achkar T, Luo L, et al. The trafficking protein Tmed2/p24beta(1) is required for morphogenesis of the mouse embryo and placenta. Dev Biol 2010;341:154-66.
26. Shin JH, Park SJ, Jo DS, et al. Down-regulated TMED10 in Alzheimer disease induces autophagy via ATG4B activation. Autophagy 2019;15:1495-505.
27. Dvela-Levitt M, Kost-Alimova M, Emani M, et al. Small Molecule Targets TMED9 and Promotes Lysosomal Degradation to Reverse Proteinopathy. Cell 2019;178:521-535.e23.
28. Zhang X, Luo Y, Li Q. TMED3 Promotes Proliferation and Migration in Breast Cancer Cells by Activating Wnt/β-Catenin Signaling. Onco Targets Ther 2020;13:5819-30.
29. Zhang X, Hao HH, Zhuang HW, et al. Circular RNA circ_0008305 aggravates hepatocellular carcinoma growth through binding to miR-186 and inducing TMED2. J Cell Mol Med 2022;26:1742-53.
30. Shi-Peng G, Chun-Lin C, Huan W, et al. TMED2 promotes epithelial ovarian cancer growth. Oncotarget 2017;8:94151-65.
31. Yang J, Huang H, Xiao D, et al. Knockdown of TMED3 inhibits cell viability and migration and increases apoptosis in human chordoma cells. Int J Oncol 2021;58:15.
32. Schmid P, Cortes J, Dent R, et al. Event-free Survival with Pembrolizumab in Early Triple-Negative Breast Cancer. N Engl J Med 2022;386:556-67.
33. Danenberg E, Bardwell H, Zanotelli VRT, et al. Breast tumor microenvironment structures are associated with genomic features and clinical outcome. Nat Genet 2022;54:660-9.
34. Salemme V, Centonze G, Cavallo F, et al. The Crosstalk Between Tumor Cells and the Immune Microenvironment in Breast Cancer: Implications for Immunotherapy. Front Oncol 2021;11:610303.
35. Riaz N, Havel JJ, Makarov V, et al. Tumor and Microenvironment Evolution during Immunotherapy with Nivolumab. Cell 2017;171:934-949.e16.
36. Hollern DP, Xu N, Thennavan A, et al. B Cells and T Follicular Helper Cells Mediate Response to Checkpoint Inhibitors in High Mutation Burden Mouse Models of Breast Cancer. Cell 2019;179:1191-1206.e21.
37. Sun MS, Zhang J, Jiang LQ, et al. TMED2 Potentiates Cellular IFN Responses to DNA Viruses by Reinforcing MITA Dimerization and Facilitating Its Trafficking. Cell Rep 2018;25:3086-3098.e3.
38. Michea P, Noël F, Zakine E, et al. Adjustment of dendritic cells to the breast-cancer microenvironment is subset specific. Nat Immunol 2018;19:885-97.
39. Gu-Trantien C, Loi S, Garaud S, et al. CD4$^+$ follicular helper T cell infiltration predicts breast cancer survival. J

Clin Invest 2013;123:2873-92.
40. Noël G, Fontsa ML, Garaud S, et al. Functional Th1-oriented T follicular helper cells that infiltrate human breast cancer promote effective adaptive immunity. J Clin Invest 2021;131:e139905.
41. Ahirwar DK, Charan M, Mishra S, et al. Slit2 Inhibits Breast Cancer Metastasis by Activating M1-Like Phagocytic and Antifibrotic Macrophages. Cancer Res 2021;81:5255-67.
42. Ali HR, Provenzano E, Dawson SJ, et al. Association between CD8+ T-cell infiltration and breast cancer survival in 12,439 patients. Ann Oncol 2014;25:1536-43.
43. Byrne A, Savas P, Sant S, et al. Tissue-resident memory T cells in breast cancer control and immunotherapy responses. Nat Rev Clin Oncol 2020;17:341-8.
44. Muntasell A, Rojo F, Servitja S, et al. NK Cell Infiltrates and HLA Class I Expression in Primary HER2(+) Breast Cancer Predict and Uncouple Pathological Response and Disease-free Survival. Clin Cancer Res 2019;25:1535-45.
45. Chen Y, Zhang S, Wang Q, et al. Tumor-recruited M2 macrophages promote gastric and breast cancer metastasis via M2 macrophage-secreted CHI3L1 protein. J Hematol Oncol 2017;10:36.
46. Allard B, Pommey S, Smyth MJ, et al. Targeting CD73 enhances the antitumor activity of anti-PD-1 and anti-CTLA-4 mAbs. Clin Cancer Res 2013;19:5626-35.
47. Karyampudi L, Lamichhane P, Scheid AD, et al. Accumulation of memory precursor CD8 T cells in regressing tumors following combination therapy with vaccine and anti-PD-1 antibody. Cancer Res 2014;74:2974-85.
48. Voorwerk L, Slagter M, Horlings HM, et al. Immune induction strategies in metastatic triple-negative breast cancer to enhance the sensitivity to PD-1 blockade: the TONIC trial. Nat Med 2019;25:920-8.
49. Vranic S, Cyprian FS, Gatalica Z, et al. PD-L1 status in breast cancer: Current view and perspectives. Semin Cancer Biol 2021;72:146-54.
50. Zhang L, Sullivan PS, Goodman JC, et al. MicroRNA-1258 suppresses breast cancer brain metastasis by targeting heparanase. Cancer Res 2011;71:645-54.
51. Hong BS, Ryu HS, Kim N, et al. Tumor Suppressor miRNA-204-5p Regulates Growth, Metastasis, and Immune Microenvironment Remodeling in Breast Cancer. Cancer Res 2019;79:1520-34.

(English Language Editor: J. Jones)

Cite this article as: Fang Z, Song YX, Wo GQ, Zhou HL, Li L, Yang SY, Chen X, Zhang J, Tang JH. Screening of the novel immune-suppressive biomarkers of TMED family and whether knockdown of TMED2/3/4/9 inhibits cell migration and invasion in breast cancer. Ann Transl Med 2022;10(23):1280. doi: 10.21037/atm-22-5444

